# Evidence that GABAergic Neurons in the Preoptic Area of the Rat Brain Are Targets of 2,3,7,8-Tetrachlorodibenzo-*p*-dioxin during Development

*Linda E. Hays,*[1,2] *Clifford D. Carpenter,*[1,2,3] *and Sandra L. Petersen*[1,2,3]

[1]Department of Biology, [2]Neuroscience and Behavior Graduate Program, and [3]Molecular and Cellular Biology Graduate Program, University of Massachusetts, Amherst, Massachusetts, USA

Developmental exposure to 2,3,7,8-tetrachlorodibenzo-*p*-dioxin (TCDD) interferes with masculinization and defeminization of male sexual behaviors and gonadotropin release patterns. We previously demonstrated that the mRNA encoding the arylhydrocarbon receptor (AhR), a protein that mediates TCDD effects, is found in brain regions that control reproductive functions, most notably in the preoptic area (POA). The pattern of distribution of the *AhR* gene closely overlaps that of an enzyme necessary for γ-aminobutyric acid (GABA) synthesis, glutamic acid decarboxylase (GAD) 67. To test the hypothesis that GABAergic neurons in the POA are targets of TCDD during development, we used dual-label *in situ* hybridization histochemistry (ISHH) to colocalize GAD and AhR mRNAs in the region. In addition, we used ISHH to determine the effects of TCDD (1 μg/kg body weight, gestational day 15) on *GAD 67* gene expression in POA regions in pups examined on postnatal day 3. We found that virtually all GABAergic neurons in the POA expressed the *AhR* gene. Furthermore, GAD 67 mRNA levels were higher in females than in males in the rostral POA/anteroventral periventricular nucleus (rPOA/AVPV) and in the rostral portion of the medial preoptic nucleus (MPN). TCDD abolished sex differences in the rPOA/AVPV but had no effect in the rostral MPN. In the caudal MPN, there were no sex differences in *GAD 67* gene expression, but TCDD depressed expression specifically in males. Our findings demonstrate that GABAergic neurons in the brain are targets of TCDD and may mediate developmental effects of this contaminant on reproductive function. *Key words:* androgen, anteroventral, estradiol, GAD, glutamic acid decarboxylase, hypothalamus, periventricular, preoptic, sexual dimorphism, TCDD. *Environ Health Perspect* 110(suppl 3):369–376 (2002).

*http://ehpnet1.niehs.nih.gov/docs/2002/suppl-3/369-376hays/abstract.html*

Dioxins and related compounds are widespread toxic contaminants that persist in the environment and accumulate in the food chain. The most potent dioxin, 2,3,7,8-tetrachlorodibenzo-*p*-dioxin (TCDD), produces a wide range of toxic effects, many of which involve disruption of endocrine functions (*1–4*). It is generally accepted that the diverse toxic effects of TCDD are mediated by the arylhydrocarbon receptor (AhR) (*5,6*), a basic helix-loop-helix transcription factor with a Per-ARNT-Sim homology domain (*7–9*). Ligand-bound AhR forms a heterodimer with AhR nuclear transporter (ARNT) or ARNT2, then binds to the xenobiotic response element (XRE; also called dioxin response element, DRE) and alters transcription of target genes (*10,11*). In addition to these genomic effects, there is evidence that TCDD binding to the AhR also alters signal transduction by activating protein kinases (*12*). Thus, the mechanisms of TCDD toxicity are complex and probably involve AhR-mediated disruption of multiple cellular signaling processes.

TCDD disrupts a variety of physiological functions; however, the finding that exposure to low doses of TCDD during development permanently alters reproductive functions is of particular concern. In male Holtzman rats, perinatal exposure to TCDD partially demasculinizes sexual behaviors (*13,14*) and interferes with defeminization of both sexual behaviors (*15*) and gonadotropin release patterns (*13*). Prenatal exposure to TCDD also demasculinizes sexual behaviors and delays the onset of puberty in male Long Evans rats but does not appear to block defeminization of behaviors in this rat strain (*16*). In female rats, a single prenatal exposure to TCDD delays the onset of puberty, prolongs the time required to achieve pregnancy in continuous breeding situations, and increases the incidence of constant estrus before old age (*16–18*). How developmental exposure to TCDD produces the observed effects on reproductive functions in adulthood is not clear. However, both gonadotropin release patterns and sexual behavioral potentials of adults are established during the critical period of perinatal life when the neural substrates controlling these functions undergo sexual differentiation (*19,20*). Sexual dimorphism of the brain is established by exposure of male brains to testosterone produced by the developing testes (*21–24*) and aromatized to estradiol (E$_2$), the hormone that defeminizes and masculinizes neural functions (*25*). Interestingly, the behavioral deficits and altered gonadotropin release observed in males exposed to TCDD are reminiscent of the effects caused by administration of antiaromatase or antiestrogenic drugs

(*25–27*). Considering that TCDD appears to be antiestrogenic in some tissues (*4*), it is possible that it also interferes with estrogen action in the brain, thereby disrupting sexual differentiation of brain regions important for reproduction.

Support for the idea that TCDD may exert antiestrogenic actions in neural tissue comes from our previous work showing that AhR, ARNT, and ARNT2 mRNAs are found in several brain regions that contain estrogen receptors (*28*). Most notably, we found members of the AhR pathway in the preoptic area (POA) of the brain, a region that contains sexually dimorphic nuclei (*29,30*). Importantly, neurotransmitter systems in the POA show sex differences in adulthood as a result of perinatal steroid hormone manipulations (*31,32*). Furthermore, specific subdivisions of the POA are required for estrogen-dependent luteinizing hormone (LH) surge release (*33,34*) and for the expression of male sexual behaviors (*35,36*). Therefore, it seems likely that developmental exposure to TCDD may permanently demasculinize and feminize the male brain by interfering with estrogen action in the POA.

The neural targets that mediate the organizational effects of steroids and might also be targets of TCDD have not been clearly delineated. However, γ-aminobutyric acid (GABA)-ergic neurons throughout the adult rat brain, including regions of the POA that control reproduction, express the *AhR* gene (*37*). In addition, the promoter regions of both glutamic acid decarboxylase (*GAD*) 67 and *GAD* 65 genes contain multiple canonical XRE sequences (*38,39*). Other lines of evidence suggest that GABAergic neurons may also be targets of estrogen and play a role in differentiation of the POA. Neurons of the POA concentrate tritiated E$_2$

(*40*) and express estrogen receptor (ER)-α and ER-β mRNA (*41*). Furthermore, GABA affects neurogenesis, neural migration, and apoptosis (*42*), processes that are all influenced by steroids and involved in creating sexually dimorphic components of the POA (*43*). Taken together, this evidence supports the hypothesis that TCDD interferes with sexual differentiation of the brain by interfering with estrogen action in GABAergic neurons.

To test this hypothesis, we first examined the effects of TCDD on *GAD 67* gene expression in POA regions of male and female offspring of Holtzman rat dams. We treated dams with 1 μg TCDD/kg body weight on gestational day 15 (GD 15) to replicate conditions previously used to show that TCDD disrupts masculinization and defeminization of sexual behaviors and gonadotropin release patterns (*13*). We measured GAD 67 mRNA levels as an index of GABAergic activity because in adult rats changes in *GAD 67*, but not in *GAD 65*, gene expression are closely linked to changes in GABA release into the POA (*44*). In the present studies, we used *in situ* hybridization histochemistry (ISHH) so that we could focus on three subdivisions of the POA that lie in close proximity: *a*) the rostral POA containing the anteroventral periventricular nucleus (rPOA/AVPV), *b*) the region containing the rostralmost portion of the medial POA (mPOA), and *c*) the region containing the caudalmost mPOA. The AVPV region is critical for the induction of LH surge release by $E_2$ (*33,34*), and the caudal mPOA is a site at which androgen regulates display of male sexual behaviors (*35,36,45*).

We next used dual-label ISHH to verify that mRNAs encoding the AhR are present in GABAergic neurons of the POA of developing brains as they are in adults. We focused on the *AhR* gene because it mediates antiestrogenic effects of TCDD (*4,5*) and because our previous work demonstrates that *ARNT* and/or *ARNT2* genes are expressed in all POA regions that express the *AhR* gene (*28*). To verify that TCDD effects are not mediated by decreases in testosterone production or interference with aromatase activity, we used ISHH to measure sex differences in progestin receptor (PR) mRNA levels in the mPOA. This approach took advantage of previous findings that males have significantly higher levels of PR than females, because $E_2$ derived from aromatization of testosterone induces PR expression (*46,47*). Finally, to confirm that all pups used in the study received similar exposures to TCDD, we used ISHH to measure CYP1B1 mRNA levels in their livers. We used *CYP1B1* as a marker of exposure because it is a target gene of the AhR

(*48*). Although TCDD induction of *CYP1A1* gene expression is more robust than that of *CYP1B1*, results of preliminary studies showed that levels of *CYP1B1* gene expression in the liver of TCDD-exposed dams are more variable than those of *CYP1A1* and also more clearly correlated with pup survival rates (*49*). Thus, they appear to be a more sensitive measure of individual responsiveness to TCDD.

## Materials and Methods

### Animals and Tissue Preparation

All the animals in this study were maintained in accordance with the National Institutes of Health *Guidelines for the Care and Use of Laboratory Animals* (*50*), and the Institutional Animal Care and Use Committee of the University of Massachusetts approved all treatment protocols used.

For this study, 14 pregnant Holtzman Sprague-Dawley rats (Harlan Sprague-Dawley, Madison, WI, USA) were delivered to the Animal Care Facility at the University of Massachusetts on day 3 of gestation (GD 3). The rats were individually housed and maintained in a temperature- and light-controlled room (14:10 light:dark cycle; lights on at 0500 hr) with food and water available *ad libitum*.

Each animal was given a Keebler Golden Vanilla Wafer (Keebler Co., Elmhurst, IL, USA) and weighed daily from GD 10 through GD 14. By GD 14, rats readily consumed the cookies, usually within 5 min after they were presented. On GD 15, rats were weighed and randomly divided into two groups. One group (*n* = 7) received vanilla wafers containing TCDD (1 μg/kg; AccuStandard, Inc., New Haven, CT, USA), and the control group (*n* = 7) received wafers treated with dimethylsulfoxide (DMSO) vehicle (Sigma-Aldrich, St. Louis, MO, USA). Wafers were prepared by applying 75 μL TCDD or DMSO solution and allowing them to dry 24 hr before distribution to the rats. Each rat was closely monitored to ensure that it consumed the entire treated cookie. Dams were weighed on GD 16, 18, 19, and 20. On GD 20, it was determined that one TCDD-treated animal and two controls were no longer pregnant. In addition, one TCDD-treated dam and pups died during parturition and pups of another TCDD-treated rat did not survive longer than 24 hr. Pups from surviving litters were weighed on postnatal day 3 (PND 3; day of birth designated PND 0) and those used in this study were sacrificed by decapitation. Both heads and trunks were collected, rapidly frozen on powdered dry ice, wrapped in Parafilm, and stored in sealed containers at –80°C until cryosectioned (Leica CM3000, Nussloch, Germany).

Brains of one male pup and one female pup from each litter (five TCDD-treated and seven vehicle-treated litters) were cryosectioned at 14 μm through the entire POA, from the region containing the organum vasculosum of the lamina terminalis through the region containing the medial POA. No available brain atlas details the POA region of neonatal rats; therefore, we used an atlas of the adult brain (*51*) that shows the features we observed in tissues of PND-3 animals. The region we refer to as the rPOA/AVPV region in PND-3 animals corresponds to plates 17 and 18 of this atlas. The rostral MPN region in our studies corresponds to plate 19, and the region we termed caudal MPN includes features shown in plates 20 and 21. Cryosections 14 μm thick from the trunk region containing the liver were also obtained from each of these pups. For both brain and liver, cryosections were collected and thaw-mounted onto gelatin-coated slides (two sections/slide), allowed to dry on a warming tray at 42°C, then stored at –80°C until ISHH was performed.

### Single-Label ISHH

For these studies, brain sections from the POA of each of the animals in the study were hybridized to ^{33}P-labeled cRNA probes specific for mRNAs encoding PR or to ^{35}S-labeled cRNA probes for GAD 65 or GAD 67 mRNAs. In addition, sections containing liver were hybridized to ^{33}P-labeled cRNA probes for CYP1B1 mRNA.

*Transcription templates.* The cDNA template for probes to PR mRNA was a 550-bp BamHI-SalI cDNA fragment corresponding to bases 383–933 of the full-length clone kindly provided by O.K. Park-Sarge, University of Kentucky (Lexington, KY, USA) (*52*). For antisense cRNA transcripts, the plasmid was linearized with BamHI, and for control sense strand transcripts, the plasmid was linearized with SalI.

The template used to prepare radiolabeled cRNA probe specific for GAD 65 was an 824-bp XbaI-HindIII cDNA fragment corresponding to bases 944–1769 that we subcloned from the full-length clone (*38*) generously provided by A. Tobin, UCLA (Los Angeles, CA, USA). For antisense cRNA transcripts, the plasmid was linearized with XbaI, while HindIII was used in the preparation of templates for control sense strand transcripts.

To prepare radiolabeled cRNA probe specific for GAD 67, we used a 535-bp HindIII-SacI cDNA fragment corresponding to bases 232–769 that we subcloned from the full-length clone (*38*) provided by A. Tobin. For antisense cRNA transcripts, the plasmid was linearized with HindIII, and

for control sense strand transcripts, the plasmid was linearized with SacI.

The cDNA transcription template for CYP1B1 mRNA was a 604-bp BamHI-EcoRV cDNA fragment corresponding to bases 85–689 of the rat CYP1B1 cDNA prepared using reverse transcription–polymerase chain reaction (RT-PCR). The forward primer was 5′CATCTCAACCGCAACTC-CAA3′ and the reverse primer was 5′AGC-CTGATGGATGGCACTCT3′. PCR was performed by first mixing buffer (Life Technologies, Gaithersburg, MD, USA) with 200 pM forward and reverse primers, 200 µM dNTPs, and 1.5 mM MgCl$_2$ in a final volume of 200 µL. The mixture was heated to 94°C for 3 min in a thermal cycler before the addition of 10 U Taq polymerase. Subsequent temperature cycles were 35 cycles at 94°C for 1 min, 57°C for 1 min, 72°C for 1 min, and a final incubation at 72°C for 10 min. The PCR-generated cDNA fragments were cloned into pCRII-TOPO (Invitrogen, Carlsbad, CA, USA) and the identity was confirmed by sequencing. The plasmid was linearized with BamHI for transcription of antisense probes and with EcoRV for sense strand probes.

**In vitro** *transcription.* All cRNA probes were prepared using *in vitro* transcription methods described previously (*53,54*), with minor modifications. Briefly, for transcription of probes for PR, GAD 65, and GAD 67 mRNAs, 90 pmol (9 µM final concentration) of ^{33}P-UTP (New England Nuclear, Boston, MA, USA) were dried down in a DNA Speed Vac (Savant, Farmingdale, NY, USA) and 1.0 µg linearized template, 1× transcription buffer, 10 mM dithiothreitol (DTT), 20 U RNAsin (Promega, Madison, WI, USA), 0.5 mM ATP, CTP, and GTP, 3 µM UTP, and 10 U of RNA polymerase were added in a total volume of 10 µL. For transcription of CYP1B1 cRNA probes, 120 pmol (12 µM final concentration) of ^{33}P-UTP was used and no unlabeled UTP was added to the transcription mixture. For each reaction, the mixture was incubated for 30 min at 37°C. A second aliquot of RNA polymerase (10 U) was added, and the mixture was incubated again for 30 min at 37°C. The template was degraded with 2 U DNAse in the presence of 20 U RNAsin, 5 µM Tris HCl, 1 µM MgCl$_2$, and 0.5 µL tRNA (25 µg/µL). The radiolabeled cRNA probes were extracted with phenol/chloroform, then precipitated twice with NaCl and EtOH and resuspended in 100 µL of 1 mM EDTA and 10 mM Tris.

*Hybridization procedures.* Separate hybridization runs were conducted for each of the probes used. In studies of PR, GAD 65, and GAD 67 mRNAs, every fourth slide (~24 sections) from the POA of each pup

was included. Similarly, every fourth section containing liver tissue was included for each pup in a single hybridization run, using the CYP1B1 cRNA probe. In each run, every 12th section was hybridized to sense strand probes to verify specificity of the probe.

After warming for 10 min at room temperature, sections were processed as described previously (*55*). They were first fixed with 4% formalin–phosphate-buffered saline for 15 min, then treated with 0.25% acetic anhydride in 0.1 M triethanolamine, 0.9% NaCl (pH 8.0), dehydrated and delipidated in a series of ethanol and chloroform rinses, and rehydrated to 95% ethanol. After the sections were dried, the cRNA probes (~1 × 10$^6$ cpm) were applied to each tissue section in 25 µL of hybridization buffer. The hybridization buffer contained 2× standard saline citrate solution (2× SSC; 1× SSC = 0.15 M NaCl and 0.015 M sodium citrate, pH 7.2), 50% (v/v) formamide, 10% (w/v) dextran sulfate, 250 µg/mL tRNA, 500 µg/mL sheared single-stranded salmon sperm DNA, 1× Denhardt's solution (0.02% Ficoll, 0.02% polyvinylpyrrolidone, and 0.02% bovine serum albumin), and 200 mM freshly prepared DTT. Sections were covered with glass coverslips and incubated in humid chambers overnight at 55°C.

After hybridization, coverslips were gently removed and sections washed in two changes of 1× SSC for 10 min each on an orbital shaker at room temperature. The slides were then washed twice with 50% (v/v) formamide/2× SSC for 20 min at 52°C and rinsed twice in 2× SSC for 10 min each rinse. The slides were then incubated in RNAse buffer with 100 µg/mL of RNAse A (Roche Corporation, Indianapolis, IN, USA) at 37°C for 30 min, rinsed twice in 2× SSC for 10 min each, and then incubated in 50% formamide/2× SSC (v/v) for 20 min at 52°C. Finally, slides were rinsed quickly in distilled water, then in three separate washes of 70, 80, and 95% ethanol for 1 min each. Dried slides were apposed to Kodak BIO-MAX X-ray film (Eastman Kodak, Rochester, NY, USA) and exposed for varying times, determined from preliminary studies using a small number of test slides. Sets of identical ^{14}C standards were exposed to X-ray films in each cassette with tissue sections and were used to verify that the films did not differ. The exposure times were 72 hr for sections hybridized to CYP1B1 or PR probes, 24 hr for GAD 65 probes, and 48 hr for GAD 67 probes. Films were developed using a Konica SRX-101A film processor (Konica Corporation, Tokyo, Japan).

## Dual-Label ISHH

For dual-label ISHH studies co-localizing AhR and GAD mRNAs in cells of the POA,

we used a mixture of two ^{33}P-labeled cRNA probes for AhR and digoxigenin-labeled probes for GAD 65 and GAD 67 mRNAs. Sections from the POAs of three vehicle-treated pups were used for this study.

*Transcription templates.* The templates for preparation of radiolabeled cRNA probes for AhR mRNA were a 1.2-kb SpeI-BamHI and a 517-bp fragment of the rat AhR cDNA that we subcloned from the full-length AhR cDNA kindly provided by C. Bradfield, University of Wisconsin (Madison, WI, USA) (*56*) into pBluescript II KS+. For antisense transcripts, the plasmid containing the 1.2-kb fragment was linearized with SpeI and the plasmid containing the 517-bp fragment was linearized with BamHI.

We used three separate templates to prepare digoxigenin-labeled cRNA probes specific for GAD mRNA. GAD 65 and GAD 67 isoforms are found primarily in the same cells, and combining the cRNA probes yields a more easily detectable signal than one probe alone. Full-length clones described above were subcloned to prepare several different constructs. The first was a 628-bp fragment corresponding to bases 315–944 of the full-length GAD 65 clone. Plasmid was linearized with XbaI for antisense transcripts. The second was a 535-bp fragment corresponding to bases 232–767 of the full-length GAD 67 clone. This plasmid was linearized with HindII for antisense transcripts. The third was an 824-bp fragment corresponding to bases 944–1769 of the full-length GAD 65 clone. This plasmid was linearized with XbaI for antisense transcripts.

**In vitro** *transcription of digoxigenin-labeled cRNA probes.* ^{33}P-Labeled probes for AhR were prepared as described above for preparation of CYP1B1 cRNA probes, using 120 pmol ^{33}P-UTP with no unlabeled UTP in the reaction. Digoxigenin-UTP–labeled cRNA probes were transcribed using 1 µg linearized cDNA template, 20 U T3 polymerase (Promega), transcription buffer, 250 µM ATP, 250 µM CTP, 250 µM GTP, 50 µM UTP, 250 µM digoxigenin-UTP (Roche Corp.), 10 µM DTT, and 1 U RNAsin. This mixture was incubated for 1 hr, then an additional aliquot of 20 U T3 polymerase was added and the mixture incubated for 1 hr at 37°C. The reaction was brought to 100 µL with nuclease-free water, and the DNA template was digested with DNAse I (2 U), in the presence of 1 U RNAsin. The probe was precipitated twice with NaCl and EtOH and resuspended in a solution of 50 µL of 1 mM EDTA and 10 µM Tris.

## Dual-Label ISHH Procedure

Dual-label *in situ* hybridization was performed as described previously (*54,57*). A

mixture of radiolabeled probes ($1.5 \times 10^6$ cpm for each probe) and digoxigenin-labeled probes (~20 ng of each GAD probe) were applied to each tissue section in 25 μL of hybridization buffer containing 50% formamide, 10% dextran sulfate, 1× Denhardt's solution, 2× SSC, 500 mg/mL heparin sodium salt, and 0.5 mg/mL tRNA. Sections were hybridized under glass coverslips overnight at 55°C. After hybridization, slides were cooled and coverslips removed in 1× SSC at room temperature, then in two 20-min 2× SSC/50% formamide washes at 52°C, followed by two 1-min rinses in 2× SSC. The sections were then incubated in RNAse solution (0.5 M NaCl; 10 mM Tris, pH 8.0; 1.0 mM EDTA, pH 8.0; containing 100 mg/mL RNAse A) for 30 min at 37°C, followed by two washes in 2× SSC for 10 min each at room temperature. Next, sections were incubated in a 20-min wash of 2× SSC/50% formamide at 52°C, followed by a brief rinse in 2× SSC.

To prevent nonspecific antibody binding, we blocked tissue sections for 1 hr in 5% blocking reagent (Roche Corp.) at room temperature. After blocking, slides were washed twice in maleate buffer (0.15 M NaCl; 0.1 M maleic acid, pH 7.5) for 3 min

each wash. Sections were then incubated in antidigoxigenin conjugated to horseradish peroxidase (Roche Corp.; 1:200 in 2% blocking reagent) for 48 hr at 4°C, washed 3 times in maleate buffer for 5 min, then 3 times in TNT buffer (0.15 M Tris HCl, 0.15 M NaCl, 0.05% Triton-X) for 5 min each. Digoxigenin signal was amplified using the NEN Renaissance Kit (New England Nuclear, Boston, MA, USA) and visualized using the ABC Elite Kit (Vector Laboratories, Burlingame, CA, USA) and freshly prepared 3,3′-diaminobenzidine tetrahydrochloride solution (DAB; Sigma Chemicals, St. Louis, MO, USA). DAB solution was prepared by mixing 10 mg DAB in 50 mL 0.1 M Tris (pH 7.6), filtering the solution through Whatman #1 paper (Whatman International Ltd., Maidstone, England), and adding 8 mL of 30% hydrogen peroxide. The reaction was stopped in 0.1 M Tris and slides were dipped briefly in water and 70% ethanol.

After immunocytochemical detection of digoxigenin-labeled cRNA probes, autoradiographical detection of radiolabeled probes was carried out by dipping the sections in NTB3 emulsion (Eastman Kodak) diluted 1:1 with deionized, distilled water. Slides

were exposed for 4–6 weeks at 4°C and then developed in Dektol and Kodak fixer.

## Data Analysis

The percentage of change in body weight between GD 15 and GD 20 in TCDD-treated and control dams was determined and values were compared using Student's t-test. Body weights of both male and female pups exposed to TCDD on GD 15 were compared with those of unexposed pups using two-way analysis of variance (ANOVA) with sex and treatment as the main effects.

The effects of TCDD on *GAD*, *PR*, and *CYP1B1* gene expression in pups were evaluated by determining relative corrected film density of the autoradiographic signals on X-ray films as described previously (*53,58*). X-ray films were placed on a light box and images were obtained with a 3CCD Video Camera (Hitachi Denshi America, Ltd., Woodbury, NY, USA) and an AF Micro-Nikkor 60-mm objective lens (Nikon USA, Melville, NY, USA). Images were digitized using BioQuant Windows image analysis software (R and M Biometrics, Nashville, TN, USA), and a threshold was set to highlight pixels representing specific labeling. The region of interest was then circumscribed and the average gray level of highlighted pixels (film density) was obtained for each region. To control for possible differences in background signal among sections, we also obtained density readings for adjacent background regions. To determine background level, we set the threshold to highlight all pixels in the field over a tissue region that had no specific signal (areas containing only white matter). This value was subtracted from the value of the specific signal to obtain corrected density readings. All sections were examined using the same threshold settings so that relative treatment differences could be determined. Computer-assisted image analysis compresses film autoradiographic responses into a 255-level gray scale, of which only 60–80 gray levels fall in the range of film
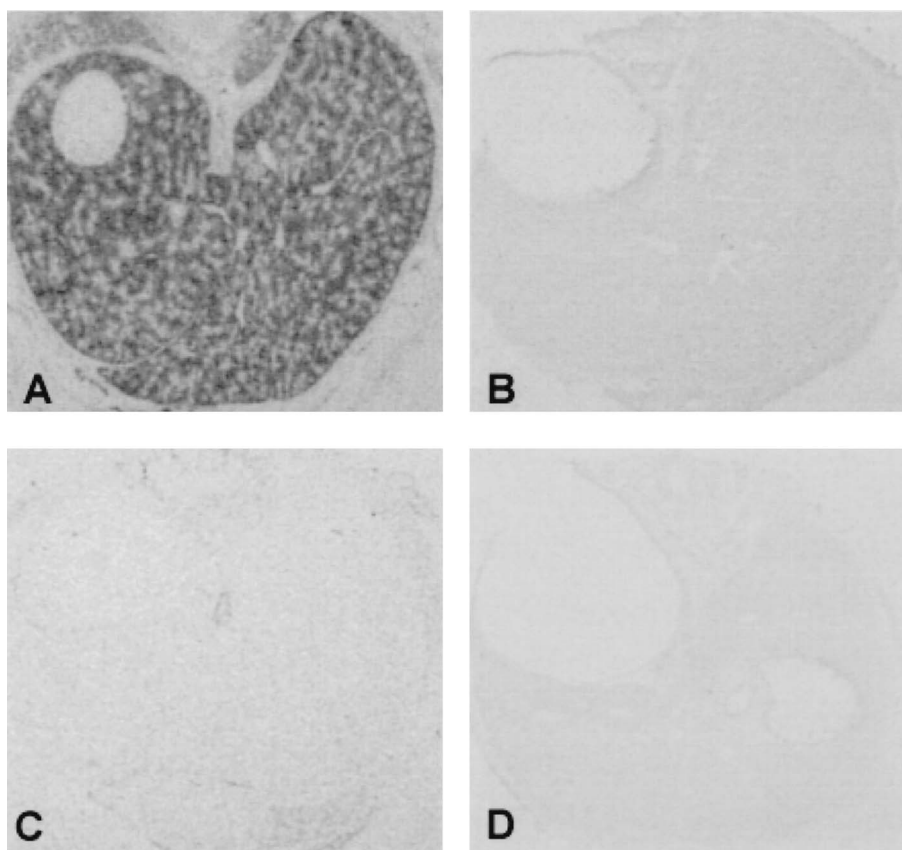


**Figure 1.** Photographs of X-ray film autoradiograms resulting from hybridizing 12-μm liver sections to ^{33}P-labeled antisense (*A,C*) or sense (*B,D*) strand cRNA probes for CYP1B1 mRNA. Tissues were obtained from PND-3 pups of dams treated with 1 μg TCDD/kg body weight (*A,B*) or vehicle (*C,D*) on GD 15.
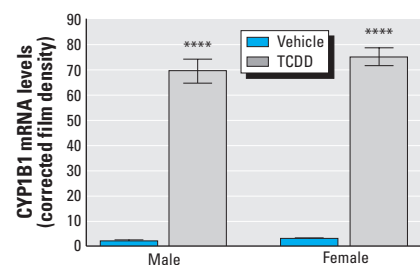


**Figure 2.** Effects of TCDD on CYP1B1 mRNA levels in liver sections from PND-3 pups exposed to TCDD (1 μg/kg po to dams; *n* = 5) or vehicle (*n* = 7) on GD 15. Bars represent mean (±SE) of autoradiographic signals corrected for background differences. ****Significantly different from vehicle-treated counterparts (*p* < 0.0001).

density. Furthermore, X-ray film responses to radioactivity are logarithmic, not linear; therefore, a change in gray scale range of 20 corresponds to as much as a 5-fold change in radioactivity in the specimen [see Vizi et al. (59) for discussion of this issue]. Thus, values obtained using this method of analysis represent relative changes in gene expression, not changes in absolute levels of mRNA, which are substantially larger. However, ISHH measurement of relative differences using film autoradiographical analysis provides the only reliable method of detecting region-specific changes in levels of gene expression.

For statistical analyses, we calculated the mean corrected density of replicate sections from individual animals in specific regions (6–8 sections/region/animal) and obtained from these a grand mean for each group and each region. These data were analyzed using two-way ANOVA, followed by Bonferroni's $t$-tests when we detected a significant interaction between sex and treatment.
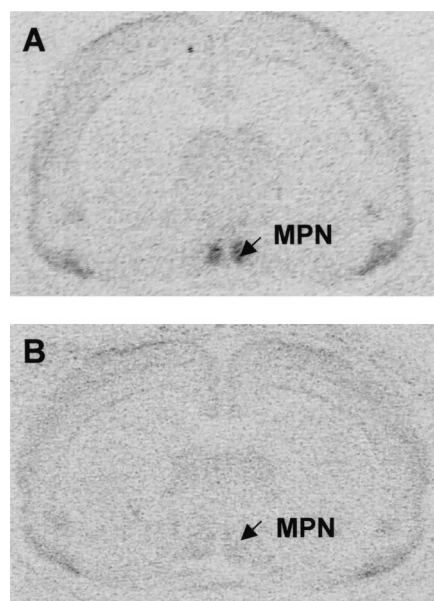
**Figure 3.** Representative film autoradiogram resulting from hybridization of MPN brain sections of untreated male (*A*) and female (*B*) PND-3 pups to $^{35}$S-labeled cRNA probes for PR mRNA.
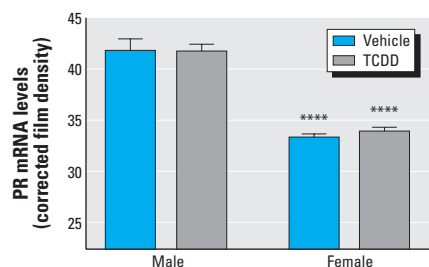
**Figure 4.** Sexual differences in PR mRNA levels in caudal MPN region of untreated PND-3 pups. Bars represent mean (±SE) of autoradiographic signals corrected for background. ****Significantly different from male counterparts (*p* < 0.0001).

## Results

We found no significant treatment effects on weights of dams at any time point and no sex differences or treatment effects on body weights of pups. We found that *CYP1B1* gene expression in pup livers (see Figure 1 for an example of autoradiographic signals) was significantly higher in TCDD-treated than in control animals (Figure 2). We found no significant differences in the expression of *CYP1B1* in pup livers between sexes. In contrast, PR mRNA levels (see Figure 3 for an example of autoradiographic signals) were significantly lower in females than in males on PND 3. These differences were not altered by TCDD exposure (Figure 4).

Results of dual-label ISHH studies (Figure 5) demonstrated that all GABAergic neurons detected in the POA contained AhR mRNA, regardless of region. Despite the uniform co-localization of GAD and AhR mRNAs, effects of TCDD on *GAD 67* gene expression differed among regions and also between sexes. Figure 6 shows examples of autoradiographic ISHH signals for GAD 67 mRNA in the rPOA/AVPV region (Figure 6A), the rostral MPN (Figure 6B), and the caudal MPN (Figure 6C). In the rPOA/AVPV region, GAD 67 mRNA levels were significantly higher in females than in males; this difference was abolished by a TCDD-induced decrease in levels detected only in females (Figure 7A). Although GAD 67 mRNA levels in the rostral MPN region were also significantly higher in females than in males, we saw no effects of TCDD (Figure 7B). Finally, in the caudal MPN (Figure 7C), we found no sex differences in

GAD 67 mRNA levels in vehicle-treated pups. However, in this region TCDD decreased levels specifically in males.

## Discussion

The results of these studies show that although virtually all GABAergic neurons in the developing POA contained AhR mRNA, TCDD altered *GAD 67* gene expression in a region-specific manner that differed between sexes. These effects do not appear to be secondary to suppression of testosterone levels, because androgen-dependent sex differences in PR gene expression in the MPN were not altered by TCDD. Furthermore, considering that TCDD decreased GAD 67 levels in both males and females, and that effects varied among regions, these changes are probably not attributable solely either to antiestrogenic effects of TCDD or to AhR activation of xenobiotic response elements in the promoter region of the *GAD 67* gene. These findings suggest that AhR activation in the brain may affect multiple signaling pathways, some of which are sex- and region-specific. Although the mechanisms responsible for disruption of *GAD 67* gene expression remain to be determined, our results clearly show that GABAergic neurons in POA regions important for gonadotropin release and male sexual behavior are targets of TCDD during development.

The present findings are the first to show that females have higher levels of GAD 67 mRNA levels than males in both the rPOA/AVPV and the caudal MPN regions but not in the more rostral MPN region. These regional differences may have
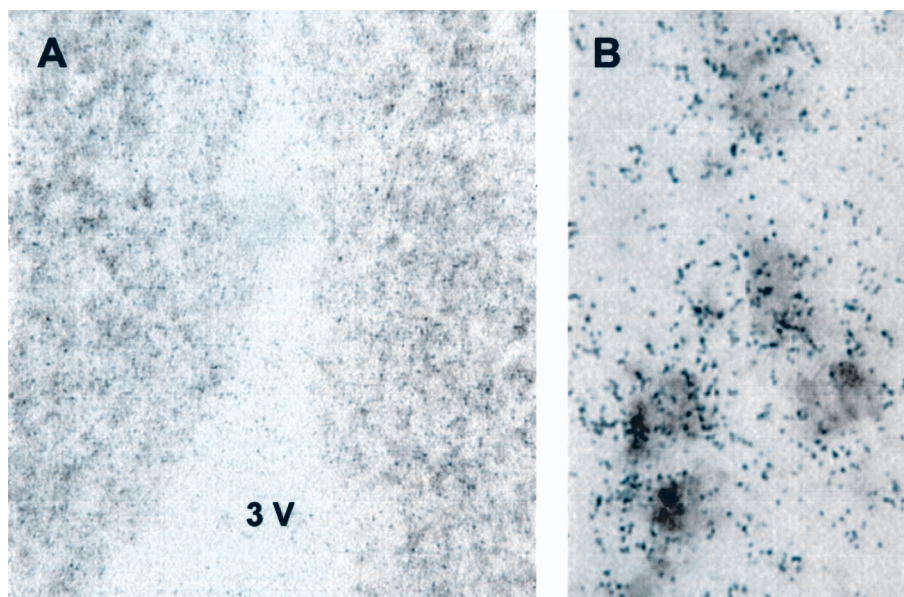
**Figure 5.** (*A*) Low-magnification (10× objective) photomicrograph showing emulsion autoradiogram resulting from hybridization of MPN tissue sections to digoxigenin-labeled cRNA probes for GAD mRNA (GAD 65 and GAD 67; brown stain over cytoplasm) and $^{33}$P-labeled probes for AhR mRNA (black silver grains). 3V, third ventricle. (*B*) Higher magnification (40× objective) of same section shown in (*A*).
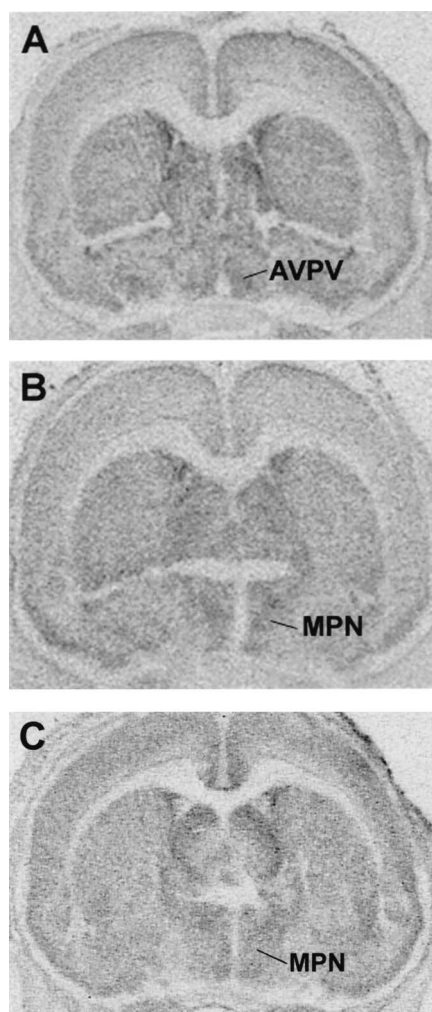
**Figure 6.** Photographs of autoradiograms resulting from hybridization of tissue sections from the (*A*) rPOA/AVPV region, (*B*) the rostral MPN, and (*C*) the caudal MPN to $^{35}$S-labeled cRNA probes for GAD 67 mRNA.

important physiological implications and emphasize the importance of considering subdivisions of the POA as functionally distinct groups of neurons. Previous work did not detect consistent sex differences in *GAD 67* gene expression in the POA of Sprague-Dawley rats on either PND 1 or 15 using ISHH or ribonuclease protection assays (*60*). In their ISHH studies, these researchers did not examine the rPOA/AVPV region and only compared single sections at the level of the sexually dimorphic nucleus of the POA, a region in which others also failed to detect sex differences in *GAD 67* gene expression (*61*). Furthermore, in the ribonuclease protection assays, they used tissue punches of the mPOA that included regions we analyzed separately in the present study (subdivisions we termed rostral and caudal MPN). It seems likely that pooling tissues could mask the region-specific sex differences we detected in GAD
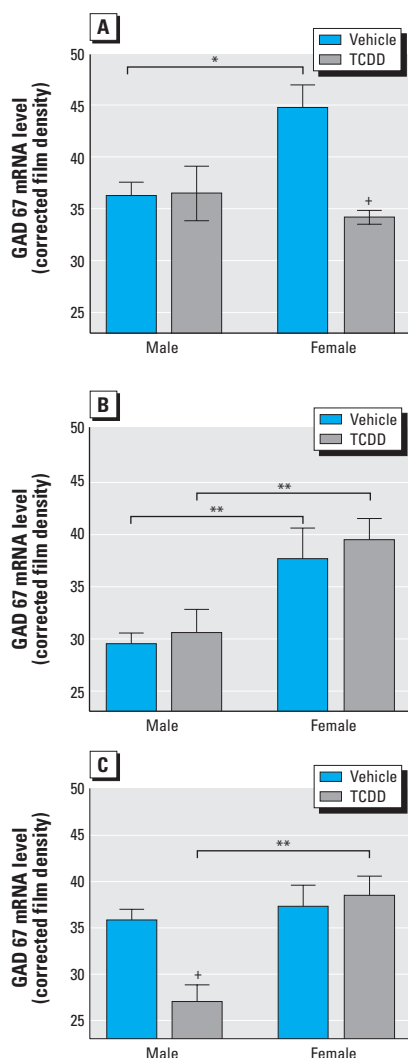


**Figure 7.** Effects of developmental exposure to TCDD (1 µg/kg po to dams on GD 15; *n* = 5) or vehicle (*n* = 7) on GAD 67 mRNA levels in male and female rats examined on PND 3. Bars represent mean (±SE) autoradiographic signals corrected for background differences. *Significantly different between sexes ($p < 0.05$). **Significantly different between sexes ($p < 0.005$). +Significantly different from vehicle-treated counterpart of same sex ($p < 0.05$).

67 mRNA levels in the caudal MPN region. Thus, methodological differences likely explain apparent discrepancies between results; nevertheless, differences in rat strain or the age at which pups were examined could also contribute to these divergent results.

*GAD 67* gene expression in the rPOA/AVPV was higher in untreated females than in male counterparts because the AVPV plays a key role in the elicitation of LH-releasing hormone and LH surge release by ovarian steroids in females. For example, microimplants of antiestrogen block the surge in $E_2$-treated ovariectomized animals (*33,34*). Likewise, lesions of this region

block the ability of progesterone to elicit LH surge release in estrogen-treated rats (*62*). Finally, specifically in the rPOA/AVPV, $E_2$ elicits temporal changes in GAD 67 mRNA levels that mark events required for the induction of LH surge release (*44*). Further studies are required to determine the mechanisms responsible for the observed sex differences and to determine whether differences in GABAergic activity during development are responsible for the sexually dimorphic structural features and functions of the AVPV in adulthood.

We found that TCDD exposure abolished sex differences in *GAD 67* gene expression in the rPOA/AVPV by specifically decreasing expression in females. Previous work shows that female rats exposed to this dose of TCDD during development show delayed onset of puberty and increased time required to achieve pregnancy in a continuous mating situation (*17,18*). In concert with the present findings, GABAergic neurons in the POA have been implicated previously in the onset of puberty. Together with the compelling evidence that GABAergic neurons of the AVPV play a role in $E_2$-dependent LH surge release and ovulation, it is reasonable to speculate that the underlying cause of disruptions in female reproductive functions is a TCDD-induced suppression of GABA synthesis during development. Nonetheless, TCDD exposure did not affect rPOA/AVPV levels of GAD 67 mRNA in males, despite previous evidence that exposure to a maternal dose of 1 µg/kg TCDD on GD 15 feminizes gonadotropin release patterns in Holtzman male rats (*13*).

Although we found no sex differences in *GAD 67* gene expression in the caudal MPN, TCDD decreased expression in this region specifically in males. This finding is intriguing in view of previous work showing that the caudal MPN is important for the expression of male sexual behaviors (*35,36*) that are altered by developmental exposure to TCDD (*13*). Unlike other regions of the POA, the caudal MPN of males has approximately 5 times as many androgen receptors as does that of females (*45*) and therefore may be the primary target for androgen action during sexual differentiation of the substrates important for masculine behaviors in adulthood. Whether TCDD-induced reduction in the activity of GABAergic neurons in the caudal MPN could interfere with behavioral masculinization is not clear, especially considering that we found no sex differences in *GAD 67* gene expression in untreated animals. However, previous work shows that perinatal treatment with the GABA$_A$ receptor antagonist picrotoxin permanently decreases male sexual behavior in adulthood (*63*). In light of this information and our finding that nearly

all AhR mRNA signal is accounted for by co-localization with GAD mRNA, TCDD-induced decreases in *GAD 67* gene expression in the caudal MPN of males could have permanent consequences, including deficits in masculine sexual behaviors.

The mechanisms underlying the variable effects of TCDD on *GAD 67* gene expression in males and females will require further research, but our present findings provide important new insights. First, we found that sex differences in PR mRNA levels in the MPN were not affected by TCDD administration. Because this sex difference depends on androgen action (*46,47*), presumably through aromatization to $E_2$, it seems unlikely that TCDD disrupted *GAD 67* gene expression by interfering with testosterone production in males. Second, we found that TCDD decreased GAD 67 mRNA levels, but it did so in both males (caudal MPN region) and females (AVPV region). Thus, effects of TCDD are probably not attributable to interference with estrogen action in the developing brain, because only males are exposed to relatively high levels of $E_2$ through local aromatization of circulating androgens. Finally, TCDD did not have the same effect on *GAD 67* gene expression in all regions, even though we found no regional differences in the percentage of co-localization of GAD and AhR mRNAs. This finding suggests that effects of TCDD do not result solely from a genomic action of the AhR on *GAD 67* gene expression. On the basis of this evidence, it seems likely that TCDD effects on *GAD 67* gene expression may involve a complex interaction among genomic effects of AhR activation, disruption of sex-specific genomic effects of steroids, and alterations in region-specific signal transduction pathways.

In summary, we found that GABAergic neurons in the POA express the *AhR* gene and that TCDD exposure during development alters *GAD 67* gene expression in a region- and sex-specific manner. Of particular importance is the finding of disruptive effects of TCDD in the rPOA/AVPV and caudal MPN. These regions play a key role in female fertility and regulation of male sexual behaviors, functions that previous work found to be disrupted when developing animals are exposed to the same dose of TCDD and the same time of administration used in the present studies. Although the mechanisms underlying TCDD disruptions of *GAD 67* gene expression are not readily apparent, they are likely to involve complex interactions of genomic and nongenomic AhR and ER pathways in GABA neurons, as well as modulation of region-specific afferent signals to GABAergic neurons.

## REFERENCES AND NOTES

1. Birnbaum LS. The mechanism of dioxin toxicity: relationship to risk assessment. Environ Health Perspect 102(suppl 9):157–167 (1994).
2. DeVito MJ, Birnbaum LS. Toxicology of dioxins and related chemicals. In: Dioxins and Health (Schecter A, ed). New York:Plenum Press, 1994;139–162.
3. Bertazzi PA, Bernucci I, Brambilla G, Consonni D, Pesatori AC. The Seveso studies on early and long-term effects of dioxin exposure: a review. Environ Health Perspect 106(suppl 2):625–633 (1998).
4. Safe S, Wang F, Porter W, Duan R, McDougal A. Ah receptor agonists as endocrine disruptors: antiestrogenic activity and mechanisms. Toxicol Lett 102–103:343–347 (1998).
5. Poland A, Knutson JC. 2,3,7,8-Tetrachlorodibenzo-*p*-dioxin and related aromatic hydrocarbons: examination of the mechanisms of toxicity. Annu Rev Pharmacol Toxicol 22:517–554 (1982).
6. Safe SH. Comparative toxicology and mechanism of action of polychlorinated dibenzo-*p*-dioxins and dibenzofurans. Annu Rev Pharmacol Toxicol 26:371–399 (1986).
7. Burbach KM, Poland A, Bradfield CA. Cloning of the Ah-receptor cDNA reveals a distinctive ligand-activated transcription factor. Proc Natl Acad Sci U S A 89:8185–8189 (1992).
8. Ema M, Sogawa K, Watanabe Y, Chujoh Y, Matsushita N, Gotoh O, Funae Y, Fujii-Kuriyama Y. cDNA cloning and structure of mouse putative Ah receptor. Biochem Biophys Res Commun 184:246–253 (1992).
9. Dolwick KM, Schmidt JV, Carver LA, Swanson HI, Bradfield CA. Cloning and expression of a human Ah receptor cDNA. Mol Pharmacol 44:911–917 (1993).
10. Whitlock JP Jr. Induction of cytochrome P4501A1. Annu Rev Pharmacol Toxicol 39:103–125 (1999).
11. Gu Y-Z, Hogenesch JB, Bradfield CA. The PAS superfamily: sensors of environmental and developmental signals. Annu Rev Pharmacol Toxicol 40:519–561 (2000).
12. Matsumura F. How important is the protein phosphorylation pathway in the toxic expression of dioxin-type chemicals? Biochem Pharmacol 48(2):215–224 (1994).
13. Mably TA, Moore RW, Goy RW, Peterson RE. *In utero* and lactational exposure of male rats to 2,3,7,8-tetrachlorodibenzo-*p*-dioxin. 2: Effects on sexual behavior and the regulation of luteinizing hormone secretion in adulthood. Toxicol Appl Pharmacol 114:108–117 (1992).
14. Bjerke DL, Peterson RE. Reproductive toxicity of 2,3,7,8-tetrachlorodibenzo-*p*-dioxin in male rats: different effects of *in utero* versus lactational exposure. Toxicol Appl Pharmacol 127:241–249 (1994).
15. Bjerke DL, Brown TJ, MacLusky NJ, Hochberg RB, Peterson RE. Partial demasculinization and feminization of sex behavior in male rats by *in utero* and lactational exposure to 2,3,7,8-tetrachlorodibenzo-*p*-dioxin is not associated with alterations in estrogen receptor binding or volumes of sexually differentiated brain nuclei. Toxicol Appl Pharmacol 127:258–267 (1994).
16. Gray LE Jr, Ostby J, Wolf C, Miller DB, Kelce WR, Gordon CJ, Birnbaum L. Functional developmental toxicity of low doses of 2,3,7,8-tetrachlorodibenzo-*p*-dioxin and a dioxin-like PCB (169) in Long Evans rats and Syrian hamsters: reproductive, behavioral and thermoregulatory alterations. Organohalogen Compounds 25: 33–38 (1995).
17. Gray LE Jr, Ostby JS. *In utero* 2,3,7,8-tetrachlorodibenzo-*p*-dioxin (TCDD) alters reproductive morphology and function in female rat offspring. Toxicol Appl Pharmacol 133:285–294 (1995).
18. Gray LE Jr, Wolf C, Mann P, Ostby JS. *In utero* exposure to low doses of 2,3,7,8-tetrachlorodibenzo-*p*-dioxin alters reproductive development of female Long Evans hooded rat offspring. Toxicol Appl Pharmacol 146:237–244 (1997).
19. Barraclough CA. Modifications in the CNS regulation of reproduction after exposure of prepubertal rats to steroid hormones. Recent Prog Horm Res 22:503–539 (1966).
20. Flerko B, Petrusz P, Tima L. On the mechanisms of sexual differentiation of the hypothalamus. Factors influencing the "critical period" of the rat. Acta Biol 18(1):27–36 (1967).
21. Barraclough CA, Turgeon JL. Ontogeny of development of the hypothalamic regulation of gonadotropin secretion: effects of perinatal sex steroid exposure. Symp Soc Dev Biol 33:255–273 (1975).
22. MacLusky NJ, Naftolin F. Sexual differentiation of the central nervous system. Science 211:1294–1303 (1981).
23. Jacobson C, Davis F, Gorski R. Formation of sexually dimorphic nucleus of the preoptic area: neuronal growth, migration, and changes in cell number. Dev Brain Res 21:7–18 (1985).
24. vom Saal FS, Montano MM, Wang MS, Sexual differentiation in mammals. In Chemically Induced Alterations in Sexual and Functional Development: The Wildlife-Human Connection (Colborn T, Clement C, eds). Princeton, NJ:Princeton Scientific Publications, 1992;17–83.
25. McEwen BS, Lieberburg I, Chaptal C, Krey L. Aromatization: important for sexual differentiation of neonatal rat brain. Horm Behav 9:249–263 (1977).
26. McDonald PG, Doughty C. Androgen sterilization in the neonatal female rat and its inhibition by an estrogen antagonist. Neuroendocrinology 13:182–188 (1973).
27. MacLusky NJ, Philip A, Hurlburt C, Naftolin F. Estrogen formation in the developing rat brain: sex differences in aromatase activity during early post-natal life. Psychoneuroendocrinology 10(3):355–361 (1985).
28. Petersen SL, Curran MA, Marconi SA, Carpenter CD, Lubbers LS, McAbee MD. Distribution of mRNAs encoding the arylhydrocarbon receptor (AhR), arylhydrocarbon receptor nuclear translocator (ARNT) and ARNT2 in the rat brain and brain stem. J Comp Neurol 427:428–439 (2000).
29. Gorski RA, Gordon JH, Shryne JE, Southam AE. Evidence for a morphological sex difference within the medial pre-optic area of the rat brain. Brain Res 148:333–346 (1978).
30. Simerly RB, Swanson LW, Gorski RA. The distribution of monoaminergic cells and fibers in a periventricular preoptic nucleus involved in the control of gonadotropin release: immunohistochemical evidence for a dopaminergic sexual dimorphism. Brain Res 330(1):55–64 (1985).
31. Simerly RB, Swanson LW, Gorski RA. Reversal of the sexually dimorphic distribution of serotonin-immunoreactive fibers in the medial preoptic nucleus by treatment with perinatal androgen. Brain Res 340(1):91–98 (1985).
32. Simerly RB, Swanson LW, Handa RJ, Gorski RA. Influence of perinatal androgen on the sexually dimorphic distribution of tyrosine hydroxylase-immunoreactive cells and fibers in the anteroventral periventricular nucleus of the rat. Neuroendocrinology 40(6):501–510 (1985).
33. Petersen SL, Barraclough CA. Suppression of spontaneous LH surges in estrogen-treated ovariectomized rats by microimplants of antiestrogen into the preoptic brain. Brain Res 484:279–289 (1989).
34. Petersen SL, Cheuk C, Hartman RD, Barraclough CA. Medial preoptic microimplants of the antiestrogen, keoxifene, affect luteinizing hormone-releasing hormone mRNA levels, median eminence luteinizing hormone-releasing hormone concentrations and luteinizing hormone release in ovariectomized, estrogen-treated rats. J Neuroendocrinology 1:279–289 (1989).
35. Gray P, Brooks PJ. The effect of lesion location within the medial preoptic-anterior hypothalamic continuum on maternal and male sexual behaviors in female rats. Behav Neurosci 98:703–711 (1984).
36. Sachs BD, Meisel RL. The physiology of male sexual behavior. In: The Physiology of Reproduction (Knobil E, Neill JD, eds). New York:Raven Press, 1988;1393–1485.
37. Laroche JaSP. Unpublished data.
38. Erlander MG, Tillakaratne NJ, Feldblum S, Patel N, Tobin AJ. Two genes encode distinct glutamate decarboxylases. Neuron 7(1):91–100 (1991).
39. Pinal CS, Cortessis V, Tobin AJ. Multiple elements regulate GAD65 transcription. Dev Neurosci 19(6):465–475 (1997).
40. Flugge G, Oertel WH, Wuttke W. Evidence for estrogen-receptive GABAergic neurones in the preoptic/anterior hypothalamic area of the rat brain. Neuroendocrinology 43:1–5 (1985).
41. McIntyre T, Hrabovszky E, Petersen SL. Unpublished data.
42. Varju P, Katarova Z, Madarasz E, Szabo G. GABA signalling during development: new data and old questions. Cell Tissue Res 305:239–246 (2001).
43. Tobet SA, Hanna IK. Ontogeny of sex differences in the mammalian hypothalamus and preoptic area. Cell Mol Neurobiol 17(6):565–601 (1997).
44. Curran-Rauhut MA, Petersen SL. Regulation of glutamic acid decarboxylase 65 and 67 gene expression by

ovarian steroids: identification of two functionally distinct populations of GABA neurons in the preoptic area. J Neuroendocrinol 14(4):310–317 (2002).

45. Lisciotto CA, Morrell JI. Sex differences in the distribution and projections of testosterone target neurons in the medial preoptic area and the bed nucleus of the stria terminalis of rats. Horm Behav 28:492–502 (1994).

46. Wagner CK, Nakayama AY, DeVries GJ. Role of testosterone, estrogen and progesterone in the sexual differentiation of the rat medial preoptic nucleus. Soc Neurosci Abstr 24:550 (1998).

47. Wagner CK, Nakayama AY, De Vries GJ. Potential role of maternal progesterone in the sexual differentiation of the brain. Endocrinology 139(8):3658–3661 (1998).

48. Sutter TR, Tang YM, Hayes CL, Wo YY, Jabs EW, Li X, Yin H, Cody CW, Greenlee WF. Complete cDNA sequence of a human dioxin-inducible mRNA identifies a new gene subfamily of cytochrome P450 that maps to chromosome 2. J Biol Chem 269(18):13092–13099 (1994).

49. Hays L, Petersen SL. Unpublished observations.

50. Guide for the Care and Use of Laboratory Animals. Washington, DC:National Academy Press, 1996.

51. Swanson LW. Brain Maps: Structure of the Rat Brain, 2nd ed. Amsterdam:Elsevier, 1998;267.

52. Park O-K, Mayo KE. Transient expression of progesterone receptor messenger RNA in ovarian granulosa cells after the preovulatory luteinizing hormone surge. Mol Endocrinol 5:967–978 (1991).

53. Petersen SL, Keller ML, Carder SA, McCrone S. Differential effects of estrogen and progesterone on levels of POMC mRNA levels in the arcuate nucleus: relationship to the timing of LH surge release. J Neuroendocrinol 5:643–648 (1993).

54. Petersen SL, McCrone S. Use of dual-label in situ hybridization histochemistry to determine the receptor complement of specific neurons. In: In Situ Hybridization Applications to Neurobiology (Valentino KL, Eberwine JJ, Barchas JD, eds). New York:Oxford University Press, 1993;78.

55. Petersen SL, Gardner E, Adelman J, McCrone S. Examination of steroid-induced changes in LHRH gene transcription using $^{33}$P- and $^{35}$S-labeled probes specific for intron 2. Endocrinology 137:234–239 (1996).

56. Carver LA, Hogenesch JB, Bradfield CA. Tissue specific expression of the rat Ah-receptor and ARNT mRNAs. Nucleic Acids Res 22(15):3038–3044 (1994).

57. Petersen SL, McCrone S, Coy D, Adelman JP, Mahan LC. GABA$_A$ receptor subunit mRNAs in cells of the preoptic area: colocalization with LHRH mRNA using dual-label in situ hybridization histochemistry. Endocr J 1:29–34 (1993).

58. Petersen SL, LaFlamme K. Progesterone increases levels of mu opioid receptor mRNA in the preoptic region and arcuate nucleus of ovariectomized, estradiol-treated female rats. Mol Brain Res 52:32–37 (1997).

59. Vizi S, Palfi A, Hatvani L, Gulya K. Methods for quantification of in situ hybridization signals obtained by film autoradiography and phosphorimaging applied for estimation of regional levels of calmodulin mRNA classes in the rat brain. Brain Res Protocols 8:32–44 (2001).

60. Davis AM, Grattan DR, Selmanoff M, McCarthy MM. Sex differences in glutamic acid decarboxylase mRNA in neonatal rat brain: implications for sexual differentiation. Horm Behav 30:538–552 (1996).

61. Gao B, Moore RY. The sexually dimorphic nucleus of the hypothalamus contains GABA neurons in rat and man. Brain Res 742:163–171 (1996).

62. Wiegand SJ, Terasawa E. Discrete lesions reveal functional heterogeneity of suprachiasmatic structures in regulation of gonadotropin secretion in the female rat. Neuroendocrinology 34:395–404 (1982).

63. Silva MR, Oliveira CA, Felicio LF, Nasello AG, Bernardi MM. Perinatal treatment with picrotoxin induces sexual, behavioral, and neuroendocrine changes in male rats. Pharmacol Biochem Behav 60(1):203–208 (1998).